aerospace

MDPI

Article

Corrosion Prevention and Control for Electrical Products of Reusable Launch Vehicles: A Life-Cycle Framework Spanning Design, Manufacturing, Testing, Operation, and Maintenance

Ning Wang [1,2,*], Bohan Zhang [3] and Yang Miao [4]

[1] Unmanned System Research Institute, Northwestern Polytechnical University, Xi'an 710072, China
[2] Beijing Institute of Astronautical Systems Engineering, Beijing 100076, China
[3] China Academy of Space Technology (CAST), Beijing 100094, China; han872004@163.com
[4] School of Mechanical and Energy Engineering, Beijing University of Technology, Beijing 100124, China; miaoyang@bjut.edu.cn
* Correspondence: wangningstef@163.com

Abstract

Electrical products of reusable launch vehicles (RLVs) face corrosion problems that expendable rockets never encounter: sea/land recovery introduces salt-fog and damp-heat exposure; repeated flights bring thermal-cycling-driven "breathing" condensation; and the "recover–refurbish–refly" mode makes corrosion damage accumulate across missions. Current standards (e.g., the salt-fog/damp-heat tests of GJB 150 and MIL-STD-810) target single-stress qualification of expendable products and lack reuse-oriented cumulative-damage criteria. This paper proposes a life-cycle corrosion prevention and control system for RLV electrical products covering five phases—design, manufacturing, testing, operation, and maintenance—including exposure-class-driven finish/coating/sealing selection, ionic-contamination control, combined-stress testing, post-recovery desalting, corrosion-specific inspection, and SCC screening of metallic housings and fasteners. A mechanism-specific state-model framework is then introduced: each corrosion mechanism is assigned its own drivers and inspectable state variable, state limits are converted to normalized life-consumption fractions, and failure/limit life is distinguished from operationally allowable life. Connector fretting corrosion is modeled with an environmental acceleration factor that preserves mechanical wear in dry enclosures. A flight-heritage data-acquisition board is used only as a case-study application, not as flight validation of corrosion behavior. The illustrative calculation shows how contact-resistance data, vibration-derived cycle counts, and operational thresholds can be linked, while Monte Carlo uncertainty propagation demonstrates the sensitivity of absolute life estimates and precludes a definitive mechanism ranking. The main contribution is therefore a reproducible method and calibration pathway for incorporating corrosion into RLV reuse decisions; product-specific test and inspection data remain necessary for validated life predictions.

Keywords: conformal coating; corrosion prevention and control; cumulative damage; electrical products; fretting corrosion; life cycle; reusable launch vehicle; reuse decision; surface protection

Check for updates

Academic Editor: Jae Hyun Park

Received: 13 September 2026
Revised: 30 October 2026
Accepted: 31 October 2026
Published: 5 November 2026

Copyright: © 2026 by the authors. Licensee MDPI, Basel, Switzerland. This article is an open access article distributed under the terms and conditions of the Creative Commons Attribution (CC BY) license.

1. Introduction

Reusable launch vehicles (RLVs) greatly reduce the cost of access to space through first-stage recovery and reflight, and have become a major development trend of space

transportation systems [1]. Reuse imposes requirements on rocket-borne electrical products (electronic units and boards for data acquisition, control, telemetry, power distribution, etc.) that are fundamentally different from those of expendable rockets: products are no longer "discarded after one flight" but undergo repeated cycles of "flight–recovery–inspection–refurbishment–reflight". In this mode, **corrosion changes from a slow variable negligible in a single mission into a cumulative damage source that limits the number of reuses**.

The corrosion problem of RLV electrical products is driven by three factors that expendable rockets do not have:

1. **Severe corrosive-media exposure introduced by the recovery environment.** Sea splashdown or sea-platform recovery exposes products directly to salt fog, seawater spray, and even short-term immersion; land recovery (landing sites) also involves sand, humidity, and diurnal dew condensation. Although the products are installed inside the vehicle's equipment bay rather than in direct contact with seawater, the bay is not watertight: marine atmosphere and spray can enter through depressurization venting paths and inter-compartment gaps, and short-term water ingress may even occur under splashdown conditions. Chloride salts such as NaCl are among the strongest corrosion promoters for electronic equipment [2].
2. **"Breathing" condensation driven by repeated thermal cycling.** Electrical products experience, together with the vehicle, repeated cycles of ground storage (ambient temperature and humidity), launch ascent (rapid decompression and cooling), and on-orbit/re-entry (large temperature swings). The air inside non-hermetic equipment "breathes" with temperature and pressure changes; moisture enters and condenses on cold surfaces. With every flight the condensation–evaporation cycle repeats once, and the corrosion media (Cl^-, ionic residues) are progressively concentrated [3].
3. **Multi-stress coupling.** Vibration, thermal cycling, and damp heat act simultaneously: vibration produces fretting at connector contact interfaces, damaging contact platings, exposing the base metal, and accelerating oxidation (fretting corrosion) [4,5]; thermal cycling generates fatigue cracks in coatings/platings that open paths for moisture and salt; damp heat and salt fog then initiate electrochemical corrosion at these defects. A product qualified under single stresses may fail rapidly under combined stresses [6].

At the same time, the reuse mode requires **quantitative cumulative management** of corrosion damage: every flight/recovery contributes an increment of corrosion damage, and the maintenance phase must answer "how many more flights are allowed"—an extension of reuse-management frameworks such as NASA's reuse readiness level (RRL) into the corrosion dimension [7]. The RRL is used here only as a conceptual analogy from software release/reuse management; for hardware-oriented reusable launch operations, maintenance, and remaining-life assessment, we additionally rely on O'Malley's reusable-component qualification accounting, informed maintenance for reusable launch systems, and launch-vehicle recovery-and-reuse practice [8–10]. This follows the same logic as the reuse management of solder thermal fatigue and structural fatigue, but the current standards system leaves an obvious gap:

- The salt-fog and damp-heat tests of GJB 150A/MIL-STD-810H are **qualification-type** single-stress tests and give no relationship between cumulative damage and allowable reuse flights [11,12];
- Conformal-coating standards such as IPC-CC-830 address **material-level** qualification of coatings and do not cover product-level life-cycle management [13];
- Existing reusability studies of RLV electronic products (e.g., our previous work on a flight-heritage board [14]) focus on solder thermal fatigue and explicitly list "cu-

mulative degradation from post-recovery corrosion/salt-fog exposure" as a not-yet-modeled limitation.

To close this gap, this paper does three things:

(1) It systematically reviews the corrosion environment profile and failure mechanisms of RLV electrical products and proposes a corrosion prevention and control system covering the five phases of **design, manufacturing, testing, operation, and maintenance**;
(2) It establishes **mechanism-specific corrosion state models** and connects their state limits to life-consumption fractions and operational reuse thresholds, so that corrosion and fatigue can be assessed within one decision structure without assuming a universal linear corrosion-rate law;
(3) It provides a **case-study application** on a flight-heritage rocket data-acquisition board (108.25 mm × 108.25 mm six-layer FR4 with ceramic PGA/LCC devices and board-to-board connectors), including an illustrative calculation, sensitivity analysis, and uncertainty propagation rather than a flight-validated life prediction.

Related Work and Positioning of This Study

The novelty of this work is best understood by comparison with five established research lines, rather than by comparison with qualification standards alone:

- **Electronics corrosion reliability.** Studies of humidity buildup, electrochemical migration, insulation-resistance degradation, and PCB time to failure provide the physical mechanisms and test methods [3,15]. They generally stop at material- or assembly-level failure criteria; they do not translate repeated recovery exposure into an allowable number of RLV reuses.
- **Fretting-corrosion life prediction.** Bryant, Wu and Pecht, Antler and Drozdowicz, and subsequent resistance–cycle models establish contact-resistance growth and its test methodology [4,5,16–18]. The present work uses these results as a submodel; it does not claim a new fretting law. Its extension is the conversion from contact-level resistance data to mission-level reuse criteria.
- **Prognostics and health management/condition-based maintenance.** CBM and remaining-useful-life frameworks connect state monitoring, degradation prediction, and maintenance decisions [19,20]. The present work adopts that logic but adds RLV-specific drivers—recovery exposure, breathing condensation, and repeated reflight acceptance—which are absent from general machinery applications.
- **Stochastic degradation and corrosion–fatigue models.** Gamma processes, Monte Carlo corrosion–fatigue assessment, and Bayesian updating provide explicit uncertainty representations [15,21–24]. These models are most reliable when calibrated by fleet or test data. The present study therefore uses uncertainty propagation only as an illustrative sensitivity tool and does not claim a validated failure probability.
- **RLV reuse management.** NASA's reuse-readiness concepts and our previous fatigue-based framework address reusable-life management [7,14], but corrosion was explicitly left as an open limitation. The present paper addresses that limitation directly.

Accordingly, the contribution is not a new corrosion mechanism or a new fretting model. It is a **mechanism-specific mapping from mission environments and inspectable corrosion states to operational RLV reuse thresholds**, together with a reproducible calibration pathway and a five-phase implementation system.

Relationship with our previous work. The present paper is the corrosion counterpart of the reusability framework established in [14], where the three-threshold reuse decision was built on solder thermal fatigue alone and "cumulative degradation from post-recovery corrosion/salt-fog exposure" was explicitly left as an open limitation. The two papers

deliberately share the same hardware platform and decision skeleton: [14] quantifies the fatigue dimension, while this paper supplies the corrosion dimension—the environmental profile, failure-mode screening, life-cycle prevention measures, mechanism-specific state models, and the conversion to operational reuse thresholds. The hardware data and fatigue results quoted from [14] serve as inputs only; the corrosion-related analysis, measures, and models of this paper are new.

2. Corrosion Environment and Failure Mechanisms of RLV Electrical Products

2.1. Environmental Profile

The life-cycle environment of RLV electrical products can be decomposed into five phases, whose corrosion-related stresses are listed in Table 1 and illustrated in Figure 1. Compared with expendable rockets, the differences concentrate in the recovery and reuse links: sea recovery brings high-grade salt-fog exposure (corresponding to the C4/C5-M marine atmospheric classes of ISO 9223 [25]), and this exposure **repeats with every flight**.

Table 1. Life-cycle environmental profile of RLV electrical products (corrosion-related).

Phase	Main Environmental Stresses	Corrosion Risk
Ground storage/assembly	Temperature/humidity swings, air pollutants, manual handling	Initial contamination buildup feeding ionic contamination and ECM
Launch ascent	Rapid decompression, cooling, vibration, acoustic	Breathing in moist air; connector fretting
On-orbit/re-entry	Large-swing thermal cycling (−40 to +95 °C for this work), vibration	Condensation–evaporation cycles; coating cracking by thermal mismatch
Recovery	**Sea salt fog/seawater spray (C4–C5-M)**, shock	Chloride deposition; water ingress into gaps and pores
Reuse inspection and storage	Cleaning, bake-out, re-storage	Cleaning residues; trapped water from incomplete drying

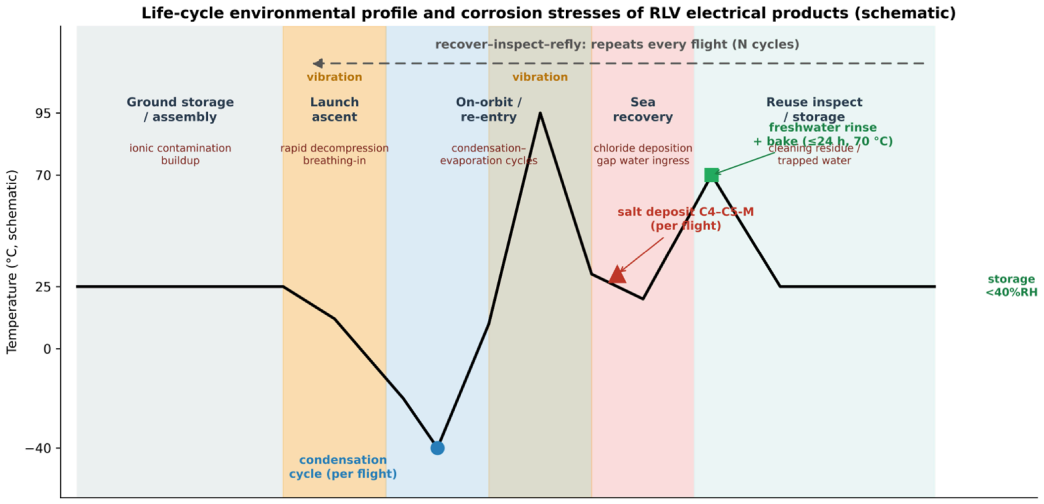


Figure 1. Life-cycle environmental profile of RLV electrical products and the corrosion stress evolution across the five phases; the recovery phase introduces repeated salt-fog exposure (E_{salt}) that accumulates with flight count N.

The transmission path of the exposure must be made explicit: the electrical products are mounted inside the vehicle's equipment bay and do not contact seawater directly, but the bay

is not a watertight structure—depressurization venting paths for the ascent phase and inter-compartment mating gaps exist permanently. After sea recovery (splashdown/platform/net capture), the marine atmosphere (C4–C5-M) and seawater spray enter the bay through these paths and deposit salt on the outer surfaces of unit housings, and several further days of marine-atmosphere exposure accumulate during the return voyage of the recovery ship. The exposure level is graded by recovery mode: sea splashdown is the highest (taken as $E_{salt} = 1$ in the model), platform/net recovery is intermediate, and land recovery is the lowest (Section 4.1); the numerical grading is an engineering estimate to be normalized against the measured chloride-deposition anchors cited below. The chloride deposition rate of marine atmospheres has been systematically measured: 150–7800 mg/(m^2·d) at the NASA KSC beachside test site and on the order of 100–600 mg/(m^2·d) in the Wenchang area of China [26,27], which can serve as measured anchors for normalizing E_{salt}; the timescale correlation between accelerated salt-fog testing and marine atmospheric exposure also has a research basis [26].

The cumulative nature of "breathing condensation" must be emphasized: moisture in the air inside non-hermetic or semi-hermetic equipment condenses on the circuit board and device surfaces after re-entry cold soak, dissolving previously deposited Cl^- to form an electrolyte film; when the temperature rises again, the water evaporates and the Cl^- concentration increases further. After N flights, the surface ionic concentration grows approximately monotonically with the number of condensation events—a key corrosion mechanism distinguishing reused products from expendable ones [3].

2.2. Major Corrosion Failure Modes

By failure location and mechanism, the corrosion failures of RLV electrical products fall into seven categories, as listed in Table 2.

Table 2. Major corrosion failure modes of RLV electrical products: mechanisms and drivers.

Failure Mode	Mechanism	RLV-Specific Driver	Typical Location
Galvanic corrosion	Dissimilar metals in contact + electrolyte film forming a galvanic cell	Mixed use of structural metals (Al/steel) and platings (Au/Sn); condensate film	Connector shells, fasteners, shield bonds
Pitting/crevice corrosion	Cl^- breaks down the passive film; occluded-cell autocatalysis	Salt deposition during sea recovery; crevices under sealing gaskets	Metal housings, grounding points
Fretting corrosion	Micro-motion at contact interfaces under vibration; plating wear and oxide-debris accumulation raising contact resistance	Multiple vibration cycles per flight; recovery shock	**Board-to-board connectors, relay contacts**
Electrochemical migration/dendrites	Metal-ion migration in a liquid film under bias; dendrite short circuits	Condensate film + operating bias; flux ionic residues	Between high-density fine-pitch solder joints
Underfilm corrosion (including filiform morphology)	Corrosion propagating beneath a coating from defects; filiform corrosion is the filamentary morphology within this category	Coating cracking under thermal cycling; insufficient edge coverage	Printed conductors under conformal coating

Table 2. *Cont.*

Failure Mode	Mechanism	RLV-Specific Driver	Typical Location
Creep corrosion	Sulfide creep over Cu/Ag surfaces toward pad edges in sulfur-bearing atmospheres	Polluted ground-storage atmospheres; immersion-silver/bare-copper surfaces	Pads, test points
Stress-corrosion cracking (SCC)	Crack initiation and growth under the combined action of a susceptible material, a corrosive environment, and sustained local tensile stress	Manufacturing residual stress, forming/crimping, assembly preload, and stress concentration; chloride or other aggressive environments [28–31]	Housings, brackets, fasteners, connector shells, and electrical terminal bolts

Among them, **fretting corrosion** is the most representative for RLVs: the contact resistance of connectors rises slowly as fretting oxide debris accumulates—a damage quantity that is **monitorable, cumulative, and directly functional**, and therefore suitable for inclusion in the reuse decision (Section 4). Bryant gave a classical account of the contact-resistance degradation mechanism of fretting corrosion [4]; Wu and Pecht provided modeling and test methods for fretting corrosion of contact interfaces [5]; and the fretting behavior of gold-plated connector contacts was systematically studied by Antler and Drozdowicz [16]. The six board-level modes and their typical sites on a flight-heritage board are illustrated in Figure 2; SCC applies to the surrounding metallic structural parts.

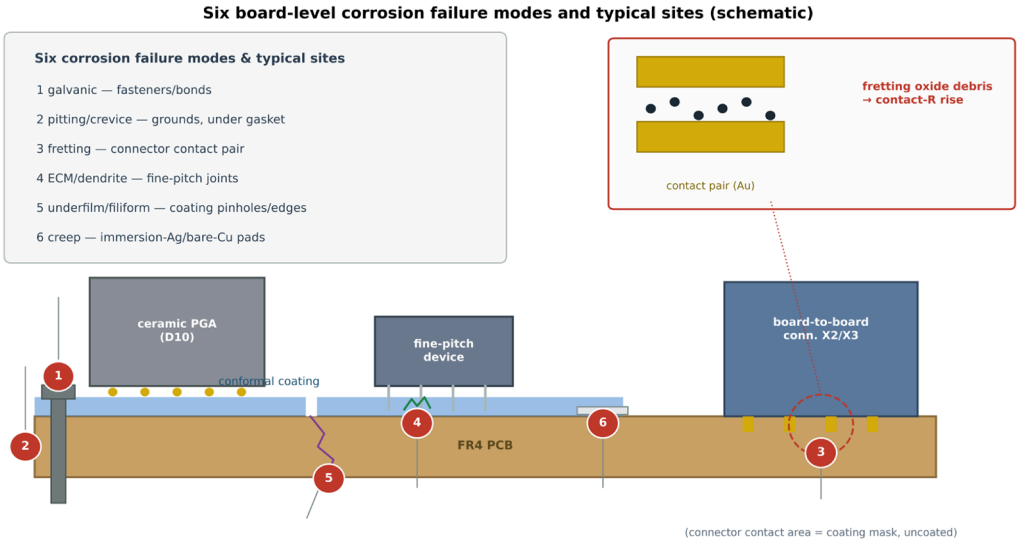


Figure 2. Six board-level corrosion failure modes and their typical sites on the flight-heritage PCB (schematic cross-section). The inset shows fretting-oxide debris raising contact resistance in a gold-plated contact pair; the board-to-board connector contact zone is left uncoated (coating mask). The labels 1–6 denote galvanic, pitting/crevice, fretting, ECM/dendrite, underfilm/filiform, and creep corrosion, respectively.

SCC is included because a globally compression- or buckling-dominated structural response does not exclude local tensile stress at a susceptible feature. Aerospace high-lock nuts and aircraft emergency-battery terminal bolts provide direct examples of cracking driven by residual/assembly stress and aggressive environments [29,30]. For RLV electrical products, the relevant objects are therefore the metallic housing, brackets, fasteners, connector shells, and terminal hardware rather than the solder joints themselves. Because product-specific material–stress–environment data are unavailable, SCC is addressed here

through mechanism screening, design controls, and inspection rather than quantitative life prediction.

Terminology is used consistently throughout the paper: **underfilm corrosion** is the general term for corrosion beneath a coating, while **filiform corrosion** denotes only its filamentary morphology; **ECM/dendrites** is treated separately because it additionally requires ionic contamination and electrical bias; **pitting and crevice corrosion** are related localized media-driven mechanisms but are not used as synonyms for underfilm corrosion.

2.3. Housing Shielding Effect and Residual Corrosion Paths

The printed-board assemblies of rocket-borne electrical products are generally mounted inside a metallic unit housing, which is the first barrier of corrosion prevention: a hermetically sealed housing can reduce board-level salt-fog exposure by an estimated one to two orders of magnitude (to be verified by housing leak-rate and witness-coupon measurements), essentially suppressing the mechanisms that depend on media supply, such as uniform corrosion and pitting. In the damage model of this paper, housing protection appears as a discount on the exposure coefficient E_{salt}: 1 for direct exposure, 0.3–0.6 for non-hermetic/vented constructions, and 0.05–0.2 for hermetic sealing. These discount factors are engineering estimates assigned by enclosure protection class; they are the starting values for the reuse decision and are to be calibrated by first-round deposition or leakage measurements on the specific product (Sections 3.4 and 6).

The housing, however, cannot reduce the corrosion risk to zero; four residual paths remain (Figure 3):

1. **Breathing effect.** A non-hermetic housing "breathes" under the rapid decompression of launch and the large temperature swings of re-entry; moist air enters and condenses on cold board surfaces—one flight, one condensation event, with Cl^- concentrated step by step (Section 2.1). Reused products experience tens of flights, and the accumulated amount is the corresponding multiple of that of an expendable product.
2. **Recovery-window exposure.** Between splashdown/landing and the opening of the compartment, salt deposits on the housing outer surface, connector tails, and cable entries; after opening, salt remains at interface locations.
3. **Seal aging with reuse.** Gaskets and sealants degrade after repeated thermal cycling and vibration, so the housing protection level declines with the number of reuses—E_{salt} should preferably be modeled as a slowly rising function of flight count rather than a constant.
4. **Weak links at feedthroughs.** Electrical connectors, vent valves, grounding posts, etc. penetrate the housing and are structural breaches of the barrier; their tails and sealing interfaces are exposed to salt fog during the recovery window, and their seals age with reuse.

It must be pointed out in particular that **fretting corrosion is not eliminated by the housing**—vibration is transmitted through the structure directly to the connector contact interfaces and cannot be shielded by the housing. The "fretting" and "corrosion" halves should, however, be distinguished: hermetic sealing blocks the external media supply, so the cavity retains only the small amount of air and moisture sealed in at closure (even less with nitrogen backfill), and oxide debris is generated more slowly than in exposed environments—the housing **decelerates rather than zeros** fretting degradation. Mechanical fretting wear itself (contact scraping, material transfer, gold-layer wear-through) requires no humid environment, and fresh wear surfaces still re-oxidize in the cavity atmosphere and accumulate flight by flight. Connectors inside housings must therefore still enter the reuse cumulative decision as fretting corrosion, and the parameters a, m, and H_{env} should be calibrated by combined-stress tests under housing-cavity atmosphere conditions

(Section 4.1). With a housing, the corrosion spectrum therefore does not "disappear" but shifts from "dominated by uniform atmospheric corrosion" to "dominated by **connector fretting corrosion plus condensation-driven underfilm corrosion/electrochemical migration**". The role of the housing is to determine which mechanisms are shielded and which remain to become limiting factors—a judgment that directly supports the mechanism screening of the case study in Section 5.

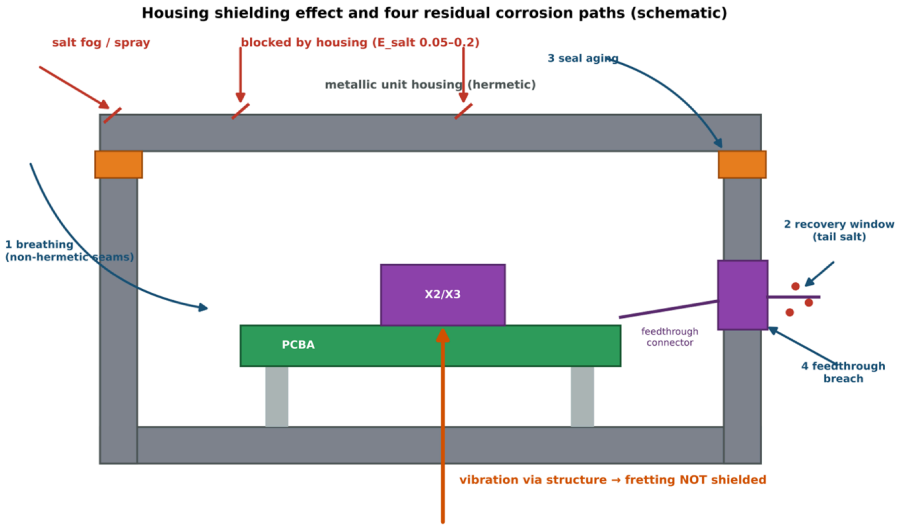


Figure 3. Housing shielding effect and the four residual corrosion channels (schematic): 1 breathing through non-hermetic seams; 2 recovery-window salt deposition at the tail; 3 gasket aging; 4 feedthrough breach; while vibration transmits through the structure unscreened.

3. Life-Cycle Corrosion Prevention and Control System

Following the principle of "prevention first, closed-loop inspection", the system is built in five phases; the overall framework is shown in Figure 4. The five phases do not duplicate existing standards: each phase starts from a qualification basis that already exists (GJB, MIL-STD, IPC), and adds the elements that RLV reuse specifically requires, as mapped in Table 3.

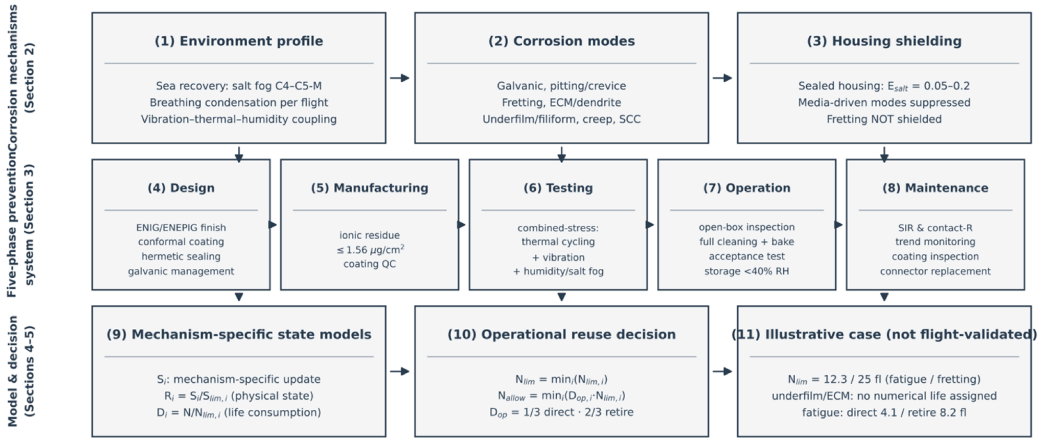


Figure 4. Life-cycle corrosion prevention and control framework for RLV electrical products: corrosion environment profile, failure modes, and housing-shielding analysis (top, Section 2); five-phase prevention measures—design, manufacturing, testing, operation, maintenance (middle, Section 3); mechanism-specific state models and operational reuse thresholds with an illustrative case application (bottom, Sections 4 and 5).

Table 3. The five-phase system mapped to gaps in existing standards and the additions of this work.

Phase	Existing Basis	Remaining Gap for RLV Reuse	Addition of This Work
Design	Coating qualification IPC-CC-830 [13]; plating series GJB 594A/QJ 450B [32,33]; dissimilar metals MIL-STD-889 [34]	No guidance on sealing–breathing balance under repeated flights, nor on recovery-exposure-driven finish selection	Exposure-class-driven finish/coating/sealing selection (Sections 2.3 and 3.1)
Manufacturing	Workmanship IPC-A-610 [35]; ionic-contamination limits [36–38]	Limits set for single use, not for flight-by-flight accumulation	Reuse-oriented cleanliness baseline feeding the damage model (Section 3.2)
Testing	GJB 150A [11]; MIL-STD-810H [12]; IPC-CC-830 [13]	Single-stress, pass/fail, no damage-calibration output	Combined-stress reuse-cycle spectrum with calibration outputs (Section 3.3)
Operation	Desalting practice of carrier-based aircraft (NAVAIR/FAA) [39–41]	No reflight acceptance gate for rocket electronics	Open-box inspection–rinse–bake–accept sequence with exposure logging (Section 3.4)
Maintenance	Rework rules IPC-7711/7721 [42]	No corrosion-metric-based reuse decision	Corrosion-specific metrics entering N_{allow} (Sections 3.5 and 4)

3.1. Design Phase

The design phase determines the majority of the inherent corrosion resistance of a product (a commonly cited engineering estimate puts it above 70%). Key points:

1. **Selection of corrosion-resistant surface finishes.** Electroless nickel immersion gold (ENIG) or electroless nickel electroless palladium immersion gold (ENEPIG) is preferred for pad finishes; bare copper and immersion silver should not be directly exposed in sulfur/salt-bearing environments (creep-corrosion sensitive). Connector contacts should be gold-plated (≥1.27 μm hard gold) rather than tin-plated—tin is fretting-corrosion sensitive, and mixed gold–tin mating actually aggravates fretting failure [4,16].
2. **Conformal coating.** Polyurethane varnish is the mainstream choice for domestic aerospace electronic products (grades such as S01-3, S31-11, and 7385, with a film thickness of 30–50 μm), applied per the process requirements of QJ 3259 [43]; coating materials are qualified per IPC-CC-830 [13]. For sea-recovery profiles the coating can be upgraded to **Parylene C**—vacuum vapor deposited, pinhole-free, dense, and with the lowest moisture vapor transmission rate, but at high cost and with difficult rework; silicone/polyurethane thick-film coatings are the second choice, silicones being suitable for high/low-temperature occasions. Coating design must define masking areas (connector contact areas, test points, heat-dissipation surfaces) [43].
3. **Sealing–breathing balance and drainage.** Unit housings are designed as "sealed + waterproof breathable membrane (ePTFE type)", blocking salt-fog ingress while balancing internal/external pressure differentials and suppressing the breathing effect; for hermetically sealed units, the housing strength and seal life are additionally verified against the repeated internal/external pressure differentials formed by rapid decompression at launch and immersion at splashdown recovery, and seals are mandatorily replaced according to the reuse count [44]. Filling the sealed cavity with dry nitrogen lowers the cavity oxygen content and can further suppress the oxidation part of connector fretting corrosion. For non-pressure-bearing, non-hermetic units, conformal

coating and drainage design take the lead, and sealing is not enforced. In all cases, the structure avoids water-accumulating pockets, with drain holes/guide surfaces and drainage slopes on all horizontal surfaces.

4. **Dissimilar-metal management.** Contact metal pairs are controlled according to the galvanic series (e.g., MIL-STD-889 [34], GJB 1720A [45]); insulating gaskets, sealants, or transition platings are inserted between pairs with large potential differences.
5. **Connector selection.** Hermetically sealed or back-potted connectors are preferred; board-to-board connectors use high-normal-force, gold-plated contact structures; mating-cycle life compatible with disassembly for recovery is considered.
6. **Inspectability design (maintenance-oriented).** Test points for insulation resistance/contact resistance are reserved; critical connectors are designed as replaceable items; board layout permits local cleaning and re-coating.
7. **SCC prevention at metallic structural parts.** For housings, brackets, fasteners, connector shells, and terminal hardware, the material–environment–stress combination is reviewed explicitly [28–31]. Measures include stress-relief treatment after forming, limits on assembly preload and crimping stress, avoidance of sharp stress concentrators, corrosion-resistant material/temper selection, and avoidance of acetic-acid-releasing sealants near susceptible metals. These controls address local tensile stress even when the global structural load is primarily compressive.

3.2. Manufacturing Phase

Manufacturing residues are the "seeds" of corrosion. Control points:

1. **Ionic-contamination control.** Post-soldering cleaning (aqueous/semi-aqueous processes); surface ionic residues are controlled by the solvent-extract resistivity (ROSE) method of GB/T 4677.22 or by ion chromatography per IPC-TM-650 2.3.25/2.3.28, with the NaCl equivalent held to $\leq$1.56 μg/cm^2 for class-3 electronic products [36–38]; direct use of no-clean processes on sea-recovery profiles is prohibited.
2. **Coating and curing quality.** Board-surface cleanliness inspection before coating; sampling inspection of coating thickness, edge coverage, and degree of cure [43]; pinhole/bubble defects accepted per IPC-A-610 [35] and GB/T 19247.1 [46].
3. **Plating process control.** Nickel/gold thickness and black-pad risk control for ENIG; gold thickness and porosity control for connector contacts, with plating selection and thickness series per GJB 594A and QJ 450B [32,33].
4. **Assembly cleanliness.** Perspiration-contamination prevention (glove/finger-cot discipline); control of workshop temperature/humidity and sulfur-bearing atmospheres, with extraneous-matter prevention per QJ 2850 [47].

3.3. Testing and Qualification Phase

The qualification philosophy must shift from single stresses to a **combined-stress joint profile**. The joint profile is compiled along the route "mission profile → stress decomposition → tailored joint spectrum → acceleration equivalence → reuse-cycle testing" (Figure 5): acceleration factors are derived from the physics of failure and must not change the failure mechanisms, and the test outputs are used to calibrate the model parameters (K_i, a, m, H_{env}, and $E_{salt}(N)$) and the monitoring baselines of Section 4.

1. **Single-stress qualification (retained).** Salt fog (GJB 150.11A/MIL-STD-810H 509.7, or the more realistic cyclic salt fog of GB/T 2423.18 [48] and the ASTM G85 modified methods [49]), damp-heat cycling (GJB 150.9A), and fungus (depending on materials) [11,12].
2. **Combined-stress test (core addition).** A joint "thermal cycling + random vibration + damp heat/salt fog" profile compiled from the real mission profile—thermal cycling

simulates launch/re-entry, vibration simulates the flight dynamic environment, and damp heat/salt fog simulates storage and recovery. Passing single-stress tests does not imply passing combined stresses: only after the coating cracks under thermal cycling + vibration will subsequent salt fog invade rapidly along the cracks [6].

3. **Coating material-level qualification.** Moisture-and-insulation resistance, fungus, and hydrolysis tests specified by IPC-CC-830 [13].
4. **Accelerated corrosion test–life correlation.** Acceleration factors are determined on the basis of the physics of failure (e.g., a temperature–humidity–bias model for electrochemical migration), converting test time into equivalent flight counts and avoiding coarse "pass/fail" qualification.
5. **Reuse-cycle testing.** The test profile should contain **multiple** "flight profile + recovery profile" cycles to simulate the cumulative effect after N reuses, rather than a single amplified profile.

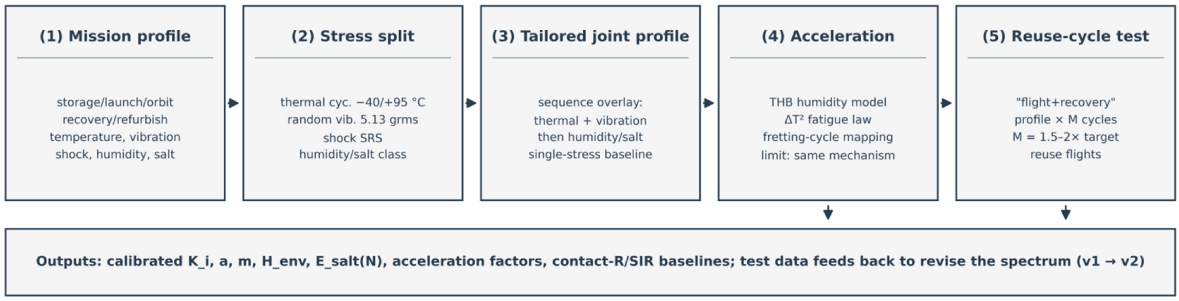


Figure 5. Combined-stress test-spectrum development flow for reuse-cycle testing (mission profile → stress decomposition → tailored combined spectrum → acceleration equivalence → reuse-cycle test), with calibrated outputs feeding the model parameters and monitoring baselines.

3.4. Operation (Recovery–Reflight) Phase

Post-recovery inspection, cleaning, and bake-out are the most critical corrosion-prevention actions for sea-recovered products, executed along the sequence "open-box inspection → cleaning → bake-out → acceptance":

1. **Comprehensive open-box inspection.** After recovery, the products are transported back to the facility (for sea recovery this can take half a month to a month, during which sea rain may still wet or soak the equipment), and the compartments are opened for a comprehensive inspection: visual examination (salt grains, water stains, corrosion traces—focusing on housing outer surfaces, feedthrough connectors, backplanes, modules, and printed boards), electrical-performance checks, and corrosion-specific checks (contact resistance, SIR, etc.; Section 3.5). Functional-performance checks alone cannot judge the corrosion state, so corrosion-specific tests must be itemized separately.
2. **Cover-opening cleaning for desalting.** As early as possible after recovery (recommended ≤24 h), surface salt deposits are rinsed with deionized water/freshwater. After splashdown/immersion, salt grains can penetrate into the unit interior—salt grains are found on housing outer surfaces, VPX backplanes, and VPX modules down to the printed boards inside modules—so covers must be opened and the internal and external surfaces of the whole unit comprehensively cleaned (deionized-water/freshwater rinse plus an electronic-cleaning process, with the resistivity and temperature of the medium standardized), focusing on crevices, connector tails, and shielded cavities. For units not immersed but humidified during marine dwell, at least the housing outer surfaces and feedthrough areas are cleaned. Freshwater-rinse desalting is established practice for carrier-based aircraft and recovered rockets [39–41].

3. **Bake-out.** After rinsing, bake at 60–80 °C until the internal dew point meets requirements, preventing trapped water from entering storage; for semi-hermetic equipment, extend the bake and supplement with dry-gas purging [40].
4. **Supplementary acceptance tests before reflight.** After cleaning, bake-out, and reassembly, supplementary high/low-temperature and random-vibration acceptance tests are performed, and only passing units are cleared for reflight. This acceptance test is the reflight gate after every recovery, distinct from the one-time qualification tests of Section 3.3.
5. **Condensation control.** Storage humidity before reflight < 40% RH, with desiccant and humidity indicator cards (HIC) [50,51]; transport cases purged with dry nitrogen or dry air.
6. **Exposure logging.** Record the sea state, exposure duration, marine dwell time, and the inspection, rinse, and bake parameters of every recovery as inputs to the damage model of Section 4.

3.5. Maintenance Phase

The maintenance phase quantifies the corrosion state as an input to the reuse decision:

1. **Corrosion-specific inspection** (performed after every recovery): visual + microscopic examination (pitting, discoloration, dendrites, coating blistering); insulation resistance/SIR (surface insulation resistance) re-measurement; **contact-resistance** re-measurement of critical connectors (four-wire method, micro-ohm-level trend); coating-integrity inspection.
2. **On-line/in-situ monitoring.** Corrosion monitoring coupons during storage (e.g., galvanic corrosion sensors, impedance-type atmospheric corrosion monitors (ACM)); leakage-current measurement on corrosion witness circuits (comb patterns) reserved on the product; for high-speed card–backplane architectures such as VPX, the SERDES built-in self-test monitors the link bit-error rate and margin on line (Section 4.3) [52].
3. **Maintenance actions.** Local re-coating of damaged coating areas; re-cleaning of contaminated areas; connector replacement based on contact-resistance trend and mating cycles; replacement of corrosion-over-limit devices per rework procedures [42].
4. **Integration with the reuse decision.** Corrosion damage metrics enter the reuse decision together with fatigue damage (next section).

4. Corrosion State Models and Integration with the Reuse Decision

4.1. Mechanism-Specific State Models and Applicability Domain

Corrosion mechanisms do not share a single multiplicative exposure law. For each mechanism i, let $S_i(N)$ be an inspectable state variable after N flights and $S_{lim,i}$ its engineering limit. A general state-update form is

$$S_i(N) = S_i(0) + \Sigma_{n=1\ldots N}\, d_i(X_{i,n}, C_{proc,i}) \quad (1)$$

where $X_{i,n}$ contains only the drivers relevant to mechanism i during flight/recovery n, and d_i is the corresponding state increment. Equation (1) is an accounting framework rather than a universal corrosion-rate law; predictive use requires mechanism-specific calibration and independent validation.

- **Electrolyte-dependent mechanisms (galvanic, pitting/crevice, underfilm corrosion, and ECM).** Here $X_{i,n}$ includes salt exposure E_{salt}, condensation count N_{cond}, time of wetness, and, for ECM, electrical bias. For a stationary exposure, a first-order increment approximation is

$$d_i = K_i \cdot {E_{salt}}^{\alpha} \cdot {N_{cond}}^{\beta} \quad (2)$$

where $K_i = k_i \cdot C_{proc,i}$ is an effective rate coefficient. The baseline rate k_i and the process/design multiplier $C_{proc,i}$ cannot be separately identified from a single life datum; separating them requires a baseline-versus-variant A/B test. The values $\alpha = \beta = 1$ are first-order assumptions, not calibrated results. Zero condensation or zero electrolyte exposure suppresses the increment only for these electrolyte-dependent modes, as intended. **Time of wetness and electrical bias are retained in the driver set and in the calibration test matrix, but are absorbed into K_i in the reduced form of Equation (2); identifying their independent effects would require an extended model with additional parameters and dedicated tests.**

- **Connector fretting corrosion.** The relevant drivers are contact motion, normal force, plating, and cavity atmosphere; salt exposure is not a necessary condition. Following Bryant's oxide-debris mechanism [4] and the fretting literature [16–18], the contact-resistance increment is

$$\Delta R(N) = a \cdot H_{env} \cdot (\Sigma_{n=1\ldots N} N_{cyc,n})^m \quad (3)$$

where a and m are fitted from resistance-versus-cycle tests, and $H_{env} \geq 1$ represents environmental acceleration. For a dry enclosure, $H_{env} = 1$ and mechanical fretting wear therefore persists. The per-flight cycle count follows the measurable chain **mission vibration PSD → contact micro-displacement (connector-level FEA or Steinberg-type board-response analysis [53]) → rainflow counting over the mission duration → effective N_{cyc}**. Equation (3) is used only before gross plating wear-through; after that transition, the parameters must be re-anchored by test.

- **Stress-corrosion cracking (SCC).** The drivers are a susceptible material, a corrosive environment, and sustained local tensile stress [28–30]. Manufacturing residual stress, forming/crimping, assembly preload, and geometric stress concentration can supply the tensile component even when the global structural response is compression- or buckling-dominated. SCC is therefore included in mechanism screening and prevention, but no quantitative SCC life model is asserted here because product-specific crack-growth data are unavailable.
- **Seal-aging correction.** For electrolyte-dependent modes, the exposure coefficient may increase with seal aging: $E_{salt}(N) = E_0 \cdot (1 + \gamma \cdot N)$, where γ is calibrated by seal thermal-cycling and vibration-aging tests [44]. Setting $\gamma = 0$ is the constant-exposure approximation used in the illustrative case.

Table 4 defines the parameters and the minimum calibration information required for reproducible use.

Table 4. Parameter definitions and calibration protocol for the mechanism-specific models.

Parameter	Physical Meaning	Required Measurement or Estimation Method
E_{salt}	Normalized marine/chloride exposure of a recovery event; reference sea splashdown = 1	Witness-coupon chloride deposition, salt-fog-equivalent dose, or ISO 9223 class [25]; class-based values are engineering priors
N_{cond}	Number of condensation–evaporation cycles per flight/recovery	Temperature, humidity, and dew-point logs; not universally equal to 1
K_i	Effective per-flight rate coefficient of electrolyte-driven mode i at reference exposure	Combined-stress tests; $K_i = k_i C_{proc,i}$. Separating k_i and $C_{proc,i}$ requires baseline-versus-variant A/B tests
α, β	Exposure exponents in Equation (2)	At least three exposure levels and two condensation levels; $\alpha = \beta = 1$ is only a first-order approximation

Table 4. *Cont.*

Parameter	Physical Meaning	Required Measurement or Estimation Method
a, m, H_{env}	Fretting resistance-law parameters and environmental acceleration	Resistance-versus-cycle tests under the mission vibration spectrum, with dry/humid comparison; a is anchored at a reference cycle count N_{ref} (not at the first flight, which would make $N_{cyc,0}$ cancel); valid before plating wear-through
$N_{cyc,0}$	Effective fretting cycles per flight	Mission PSD → contact micro-displacement FEA [53] → rainflow counting
$S_{lim,i}$	Mechanism-specific state limit	Table 5 gives engineering starting values, to be refined by product measurement history

Table 5. Monitorable metrics and engineering starting criteria for corrosion state tracking.

Mechanism	Monitored Quantity	Engineering Starting Criterion (Not a Universal Acceptance Limit)
Connector fretting corrosion	Contact resistance (four-wire method)	Warning at >50% or >2-fold rise over initial value; replace at >5 mΩ increment [4,5]
High-speed mating connectors (VPX-type card–backplane)	Link bit-error rate/link margin (SERDES built-in self-test, on-line)	Warning when the error rate exceeds threshold or margin drops >3 dB; replace when retraining/link-failure counts keep growing [52]
ECM/ionic contamination	SIR (comb pattern, 85/85 bias)	Warning at $<10^8$ Ω; ground for investigation at $<10^7$ Ω
Coating failure	Under-coating leakage current/impedance spectroscopy	Warning at one-order-of-magnitude drop in impedance modulus
Storage atmospheric corrosion	ACM corrosion current	Extrapolate remaining life at ISO 9224 rates [54]
SCC-susceptible housings, brackets, and fasteners	Visual/NDT indications, local residual-stress and preload control records	Inspect after recovery and after any evidence of coating damage, leakage, or abnormal preload [28–31]

A linear representation is required only for the **life-consumption fraction** defined in Section 4.2, not for the physical state S_i. Equation (2) is applicable only under approximately stationary exposure and in the absence of incubation or stage transitions. An incubation stage is represented by $d_i = 0$ until its end; after a transition such as passivation breakdown or plating wear-through, the rate parameters must be recalibrated. Thus, the framework does not assume that all corrosion processes are physically linear.

4.2. From State Limits to Life-Consumption Fraction and Operational Criteria

The physical damage ratio $R_i(N) = S_i(N)/S_{lim,i}$ is generally nonlinear and must be distinguished from the life-consumption fraction $D_i(N) = N/N_{lim,i}$, where $N_{lim,i}$ is the flight count at which S_i reaches $S_{lim,i}$. For the fretting model of Equation (3), with a constant per-flight cycle count $N_{cyc,0}$,

$$N_{lim,fretting} = (\Delta R_{lim}/(a \cdot H_{env}))^{1/m}/N_{cyc,0} \quad (4)$$

and the two damage representations are related by $D_{fretting} = {R_{fretting}}^{1/m}$, or equivalently $R_{fretting} = {D_{fretting}}^{m}$. A linear plot of $D_{fretting}$ is therefore fully consistent with the nonlinear resistance law.

The system limit life is governed by the earliest mechanism to reach its limit:

$$N_{lim} = \min_i(N_{lim,i}) \quad (5)$$

Equation (5) is a weakest-link comparison of limit lives, not a sum or product of damage contributions. The other mechanisms remain active inputs to inspection and maintenance; after connector replacement, re-coating, or device rework, their states and $N_{lim,i}$ are recomputed, and the controlling mechanism may change.

Limit life must further be distinguished from operationally allowable life. For an operational threshold $D_{op,i}$,

$$N_{allow} = \min_i(D_{op,i} \cdot N_{lim,i}) \quad (6)$$

where $D_{op,i} = 1/3$ gives the direct-reuse boundary and $D_{op,i} = 2/3$ gives the retirement boundary under the management convention of [14]. For these two thresholds, we use the more explicit notation $N_{direct} = \min_i(N_{lim,i}/3)$ and $N_{retire} = \min_i(2N_{lim,i}/3)$, rather than reusing N_{allow} for both. These thresholds are operational rules, not physical corrosion laws. Failure/limit life corresponds to $D_i = 1$ and must not be inserted directly as N_{allow}. Equation (6) is an engineering approximation for parallel mechanisms; shared thermal, vibration, and humidity drivers can introduce correlations, which require joint test data or a stochastic model for a fully probabilistic treatment.

4.3. Monitorable Metrics and Criteria

The state variables must be measurable, forming a model-prediction–measurement-verification loop (Table 5). The warning criteria below are engineering starting values for in-service trending, not universal acceptance limits; they should be tightened or relaxed using the product's own measurement history (Section 3.5).

4.4. Illustrative Uncertainty Propagation and Stochastic Extensions

Recent studies have used probabilistic models for PCB humidity-driven time to failure [15], stochastic corrosion–fatigue assessment [22–24], and Bayesian updating with inspection data [23]. Gamma-process and related degradation models provide further general foundations [20,21]. These approaches are most persuasive when their distributions are calibrated by product or fleet data.

Because the input distributions of the present study are not product-calibrated, absolute failure probabilities would be misleading. Monte Carlo propagation is therefore used here only as an **illustrative uncertainty analysis**: input distributions are stated explicitly, and the outputs are conditional percentiles rather than validated reliability predictions. As an example, 100,000 draws are made with $m \sim \text{Uniform}(0.3, 0.7)$, $\log_{10}N_{cyc,0} \sim \text{Uniform}(3, 5)$, and $\Delta R_{ref} = 1\ m\Omega$ at a reference cycle count $N_{ref} = 10\text{^}4$. The coefficient is computed as $a = \Delta R_{ref}/N_{ref}{}^m$. Anchoring a at the first flight would make $N_{cyc,0}$ cancel out of Equation (4); the reference-count anchor avoids that cancellation, so uncertainty in $N_{cyc,0}$ enters the lifetime distribution linearly. Under this convention, the illustrative $N_{lim,fretting}$ distribution has a median of 30.3 flights, a 5th–95th percentile interval of 2.4–426 flights, and 30.9% of draws below the fixed 12.3-flight fatigue limit. **This percentage is only a fretting-parameter and cycle-count sensitivity result with fatigue held fixed, independent inputs, and no model-error term; it is not a joint probability of the controlling mechanism under combined fatigue-and-fretting uncertainty.** Thus, even the illustrative ranking is conditional rather than definitive. After product measurements become available, the same state model can support Bayesian updating or Gamma/Wiener-process formulations without changing the reuse-decision structure.

5. Case-Study Application on Flight-Heritage Hardware

5.1. Object of Analysis

The object is the rocket-borne data-acquisition board with a real flight heritage that was analyzed for thermal fatigue in [14]: six-layer FR4, true ODB++ board outline 108.25 mm × 108.25 mm × 1.62 mm, 109 components; the full hardware description and the finite-element model are given in [14] and are not repeated here. **The flight heritage is used only to define a realistic hardware and mission context; it does not constitute flight validation of the corrosion model, because no flight-derived time series of contact resistance, SIR, chloride deposition, or coating degradation are available.** From the corrosion perspective, the critical sites (Figure 6) are different from the fatigue-critical ones: the two 51-pin board-to-board connectors X2/X3 (mating with another printed board inside the same chassis, not cabled to the housing), whose gold-plated contact zones are necessarily left uncoated and constitute the principal fretting-corrosion exposure; and the coating edges around the large ceramic packages (D10 PGA-133, D9 LCC-20, D6–D8 FIFO-32), where thermal-cycling-driven coating cracking is most likely to initiate underfilm corrosion. The board is mounted inside a sealed unit housing (connectors cabled out through sealed feedthroughs), corresponding to the "hermetic sealing + feedthroughs" exposure class of Section 2.3. Previous thermal-fatigue analysis identified D10 as the fatigue-limiting device (12.3 flights on the conservative Model-1 tier [14]); X2/X3, as structural interconnections, do not participate in the solder-joint fatigue ranking and must be evaluated separately for fretting corrosion [14].

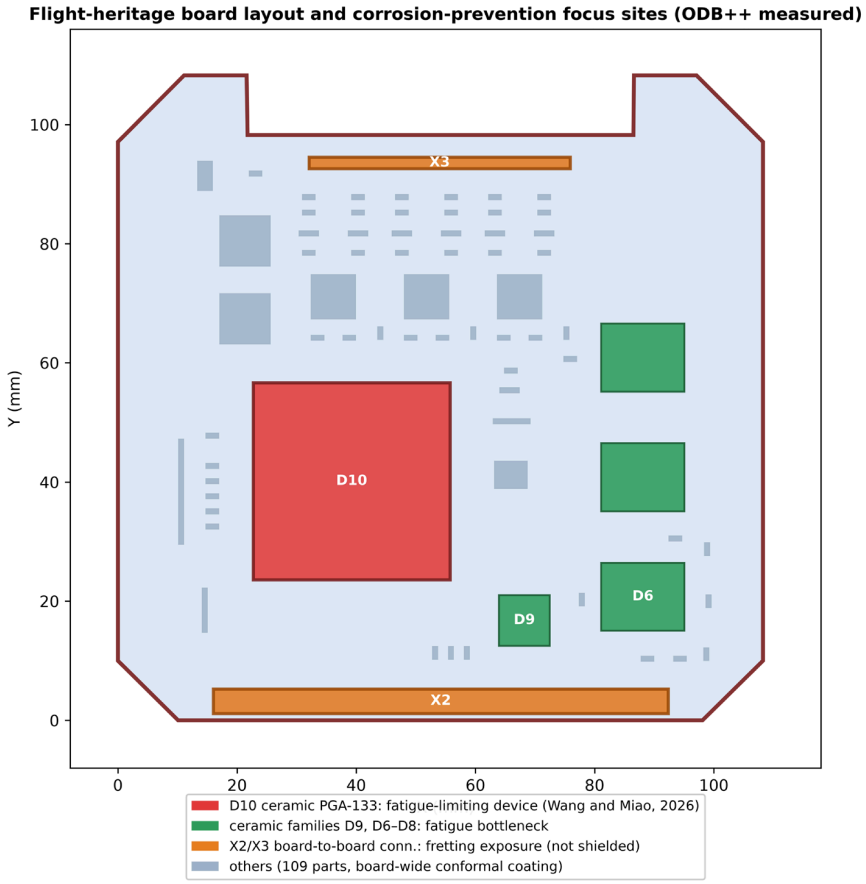


Figure 6. Layout of the flight-heritage board with corrosion-critical sites marked (ODB++ measured outline, 108.25 mm × 108.25 mm): D10 (ceramic PGA-133, the fatigue-limiting device in [14], conservative Model-1 tier 12.3 flights), the D9/D6-D8 ceramic families, and the X2/X3 board-to-board connectors (fretting-corrosion exposure unscreened by the housing).

5.2. Existing Practices and Proposed Additions in the Five Phases

The measures below mix existing operational practices with proposed additions required for calibration. They are separated to avoid implying that model-validation tests have been performed. Established workmanship controls and recovery operations provide the hardware context, but they were not instrumented as a corrosion-validation experiment. The combined-stress calibration tests and dedicated corrosion trend series are proposed procedures.

- **Design (implemented design features).** ENIG pad finish; X2/X3 selected as gold-plated contact (≥1.27 µm) high-normal-force structures; board-wide conformal coating: polyurethane varnish (30–50 µm, applied per QJ 3259 [43]) in current practice, upgradable to Parylene C (20–25 µm) for sea-recovery profiles, with connector contact areas masked; hermetically sealed unit housing with connectors cabled out through sealed feedthroughs; insulating transitions between metallic fasteners and the housing; control of assembly preload and residual stress at SCC-susceptible housings, brackets, and fasteners. These are design features, not degradation measurements.
- **Manufacturing (implemented process controls).** Post-soldering aqueous cleaning + ion-chromatography sampling (NaCl equivalent ≤ 1.56 µg/cm^2); cleanliness inspection before coating; pinhole sampling inspection after coating. These controls establish process quality but do not constitute corrosion-life validation.
- **Testing (existing qualification plus proposed calibration).** Single-stress damp-heat and cyclic salt-fog tests were performed as qualification activities. The combined "−40/+95 °C thermal cycling + random vibration + damp heat" profile with contact-resistance monitoring of X2/X3 is a **proposed calibration procedure**, not a completed corrosion-validation test.
- **Operation (existing recovery practices plus proposed logging).** Comprehensive open-box inspection after recovery, cover-opening cleaning after splashdown, bake-out, and supplementary high/low-temperature and random-vibration acceptance tests are established recovery operations; they provide context but were not instrumented as a standardized corrosion time series. Exposure logging is a proposed addition for model input.
- **Maintenance (proposed monitoring additions).** Multi-flight contact-resistance and SIR trend series, coating impedance sampling, and SCC-site inspection records are recommended monitoring additions; no such trend dataset is analyzed in this manuscript.

5.3. Illustrative Model Application and Operational Thresholds

The following calculation illustrates the model workflow; it is not a validation using corrosion-test or flight-derived degradation data. The board's flight heritage defines a realistic hardware and mission context only. The housing is assigned $E_{salt} = 0.2$ (the upper bound of the hermetic-sealing range, a conservative engineering estimate), $N_{cond} = 1$, and $\gamma = 0$. These values are assumptions for demonstration, not measured product parameters. **The 1/3 and 2/3 thresholds are used only to demonstrate compatibility with the fatigue-based framework of [14]; mechanism-specific corrosion thresholds should instead be determined by risk policy, inspection capability, and product data, and are not presumed to be universally identical to the fatigue thresholds.**

The fretting-corrosion value in Table 6 is obtained by an explicit forward calculation along the conversion chain of Section 4.1, rather than by assertion. The calculation is highly sensitive to the exponent m and to the assumed cycle count; it must therefore be interpreted as an illustrative scenario, not as a product-specific ranking of limiting mechanisms. The underfilm/ECM row is retained for inspection completeness, but no numerical limit life is

assigned because no defensible rate data are available. The corresponding parameter chain is summarized in Table 7.

Table 6. Illustrative limit lives and their translation into operational thresholds for the flight-heritage board ($E_{salt} = 0.2$, $N_{cond} = 1$, $\gamma = 0$).

Mechanism (Location)	Key Parameters and Protection State	Illustrative Limit Life N_{lim}	Direct-Reuse Boundary $N_{lim}/3$	Retirement Boundary $2N_{lim}/3$
Solder thermal fatigue (D10 ceramic PGA-133)	Engelmaier model from FEA and device data [14]; conservative Model-1 tier, ALT calibration pending	12.3 flights	4.1 flights	8.2 flights
Connector fretting corrosion (X2/X3)	Gold-plated contacts ≥1.27 µm, high-normal-force structure; unshielded vibration path; nominal calculation in the following table	25 flights	8.3 flights	16.7 flights
Underfilm corrosion/ECM (board surface)	Board-wide conformal coating + controlled ionic contamination; housing shielding $E_{salt} = 0.2$	Not assigned (no calibrated rate)	—	—

Table 7. Illustrative fretting-corrosion calculation for connectors X2/X3 (parameters assumed for demonstration and requiring product-specific calibration).

Chain Link	Parameter	Value	Basis
Threshold	ΔR_{lim}	5 mΩ	Engineering starting criterion of Table 5
Mission → cycles	Effective fretting cycles per flight $N_{cyc,0}$	~10^4	Rainflow of the contact micro-displacement history; to be measured or simulated by connector-level FEA [53]
Rate-law exponent	m	0.5 nominal (assumed sensitivity range 0.3–0.7)	Illustrative range selected for sensitivity analysis, not a directly fitted range from [17,18]
Rate constant and reference	a, H_{env}, N_{ref}	0.01 mΩ·cycle^{-m}, $H_{env} = 1$, N_{ref} = 10^4 cycles	Anchored at $\Delta R_{ref} = 1$ mΩ at the reference count N_{ref}, with $a = \Delta R_{ref}/N_{ref}^{m}$; dry-cavity environmental acceleration set to unity
Resulting limit life	$N_{lim,fretting} = (\Delta R_{lim}/(aH_{env}))^{1/m}/N_{cyc,0}$	≈ 25 flights (nominal)	Forward substitution into Equation (4)
Deterministic sensitivity	Same reference anchor, m = 0.3/m = 0.7	>200/~10 flights	Demonstrates the need to calibrate m
Illustrative uncertainty propagation	100,000 Monte Carlo draws (Section 4.4)	Median 30.3; 5th–95th percentile 2.4–426 flights; 30.9% below 12.3 flights	Conditional on the stated distributions and reference-count anchor; not a validated failure probability

Substituting the illustrative values into Equation (5) gives $N_{lim} = \min(12.3, 25) = 12.3$ flights. This is the **limit life at D = 1**, not the operationally allowable life. Applying the direct-reuse and retirement boundaries gives $N_{direct} = \min(4.1, 8.3) = 4.1$ flights and $N_{retire} = \min(8.2, 16.7) = 8.2$ flights. These quantities are kept distinct throughout the revised decision procedure.

The corresponding normalized life-consumption fractions and operational boundaries are shown in Figure 7.

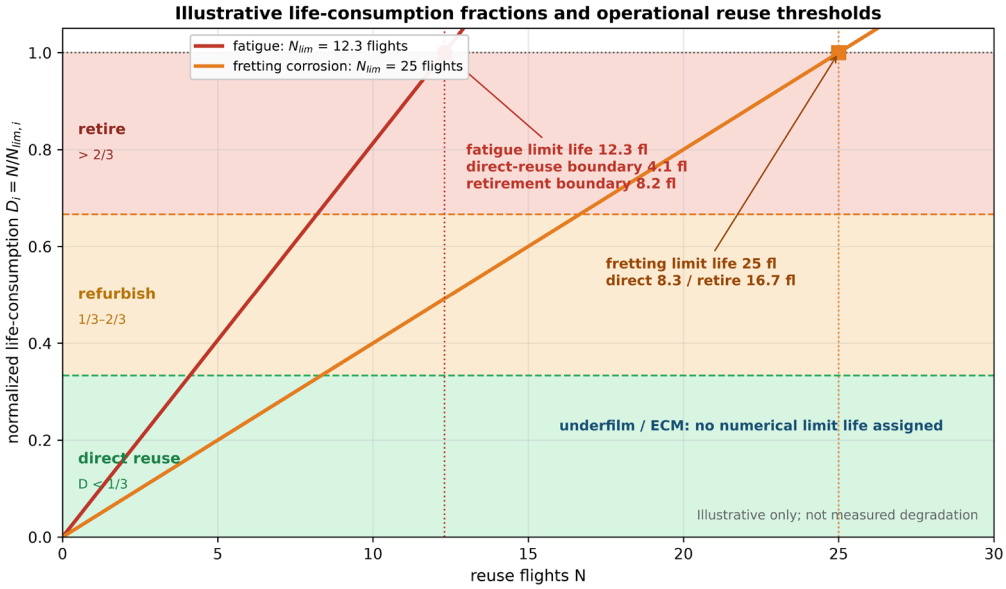


Figure 7. Illustrative normalized life-consumption fractions $D_i = N/N_{lim,i}$, not normalized resistance or experimentally measured degradation trajectories. The curves use N_{lim} = 12.3 and 25 flights for fatigue and fretting corrosion. Underfilm corrosion/ECM is not assigned a numerical limit life and is therefore not plotted. The horizontal lines are operational thresholds at D = 1/3 and D = 2/3; the fatigue limit life is 12.3 flights, while its direct-reuse and retirement boundaries are 4.1 and 8.2 flights. All inputs are illustrative.

The application illustrates three mechanism-screening points. First, housing protection suppresses the electrolyte-dependent mechanisms that dominate exposed boards. Second, fretting degradation remains possible because the mechanical vibration path is not shielded by the housing. Third, after fatigue refurbishment, another mechanism can become controlling, so corrosion and fatigue must be assessed in parallel. These are conclusions about model structure and inspection needs, not validated absolute-life predictions. SCC remains a parallel screening item for the housing, brackets, and fasteners, but is excluded from the numerical budget because no material–stress–environment-specific crack-growth data are available.

6. Discussion

1. **Model positioning.** The proposed model is an engineering state-accounting and decision framework, not a validated absolute-life predictor. Its value is to connect inspectable corrosion states with reuse decisions in the same way that fatigue states are already used. Parameters K_i, a, m, H_{env}, and the exposure variables must be calibrated by combined-stress tests and in-service measurements before predictive use.
2. **Relationship with existing standards.** The proposed system does not replace GJB 150/MIL-STD-810 qualification tests; it superimposes reuse cycling and cumulative management on top of their qualification basis—the two are related as "admission" versus "in-service management".
3. **Limitations and evidence boundary.** No product-specific corrosion-test series or flight-derived corrosion time series are available in this study. The numerical examples are therefore illustrative scenarios, and neither an absolute mechanism ranking nor a validated absolute reuse life is claimed. SCC is included in mechanism screening, design control, and inspection, but not in the quantitative budget because material–

stress–environment-specific crack-growth data are unavailable. The uncertainty distributions in Section 4.4 are also assumptions rather than fitted fleet statistics.

4. **Calibration pathway.** The literature provides mechanism-level rate laws and starting thresholds [4,5,16–18,26,27,44], but product-specific transfer coefficients—bay salt ingress, contact micro-displacement, housing leak-rate growth, and the measured re-entry vibration spectrum—must be obtained by first-round measurements or FEA. This is precisely the division of labor behind the test-spectrum development route of Section 3.3: mechanism rates come from the literature, and transfer coefficients come from measurement. After such data are collected, independent validation should compare predicted and measured state evolution before the model is used for certified reuse limits.

7. Conclusions

(1) The corrosion of RLV electrical products has three specific drivers—salt exposure from sea recovery, breathing condensation, and multi-stress coupling—and current single-stress qualification standards do not cover reuse accumulation.

(2) A corrosion prevention and control system covering the five phases of design, manufacturing, testing, operation, and maintenance is proposed. Its core measures are corrosion-resistant platings and coatings, sealing-with-breathing design, ionic-contamination control, combined-stress testing, post-recovery desalting, corrosion-specific inspections, and SCC screening of metallic housings and fasteners.

(3) Mechanism-specific state models are established for electrolyte-dependent corrosion and connector fretting corrosion. By distinguishing physical state ratios from normalized life-consumption fractions, and failure/limit life from operationally allowable life, the framework connects corrosion and fatigue within one reuse-decision structure without assuming a universal linear corrosion-rate law.

(4) The flight-heritage hardware application demonstrates the calculation and calibration workflow, including sensitivity and uncertainty propagation. It does not constitute flight validation or establish a definitive absolute-life ranking. Product-specific test and inspection data remain necessary before the framework can support certified reuse limits.

Author Contributions: Conceptualization, N.W.; methodology, N.W.; software, N.W.; validation, N.W., Y.M. and B.Z.; formal analysis, N.W.; investigation, N.W. and B.Z.; data curation, Y.M. and B.Z.; writing—original draft preparation, N.W.; writing—review and editing, N.W., Y.M. and B.Z.; visualization, N.W.; supervision, Y.M.; project administration, N.W. All authors have read and agreed to the published version of the manuscript.

Funding: This research received no external funding.

Institutional Review Board Statement: Not applicable.

Informed Consent Statement: Not applicable.

Data Availability Statement: The scripts implementing the forward evaluation of Equations (3)–(6), the sensitivity analysis of Table 7, the illustrative Monte Carlo propagation of Section 4.4, and all figure-generation scripts are available from the corresponding author upon reasonable request. The hardware data of the flight-heritage board are subject to the data policy of the owning organization and were used in the form published in [14].

Acknowledgments: During the preparation of this manuscript, the authors used an artificial intelligence (AI) assistant for manuscript formatting and typesetting, and for programming implementation. The authors reviewed and edited all output and take full responsibility for the content of this publication.

Conflicts of Interest: The authors declare no conflicts of interest.

Nomenclature

Symbol	Description	Unit/Value
$S_i(N)$	Inspectable state variable of mechanism i after N flights	mechanism-dependent
$S_{lim,i}$	Engineering limit of the state variable S_i	mechanism-dependent
d_i	Per-flight state increment of mechanism i	mechanism-dependent
$X_{i,n}$	Mechanism-specific driver set during flight/recovery n	-
E_{salt}	Normalized salt/marine exposure of a recovery event	0–1 (sea splashdown = 1)
N_{cond}	Condensation–evaporation cycles per flight	~1 (illustrative)
$C_{proc,i}$	Process/design multiplier for mechanism i	1 for baseline design
k_i	Baseline rate constant of mechanism i	calibrated by test
K_i	Effective rate coefficient, $K_i = k_i C_{proc,i}$	calibrated by test
α, β	Exposure exponents in Equation (2)	1 (first-order approximation)
R_i	Physical state ratio, $R_i = S_i/S_{lim,i}$	-
D_i	Normalized life-consumption fraction, $D_i = N/N_{lim,i}$	-
$N_{lim,i}$	Limit life of mechanism i at $S_i = S_{lim,i}$	flights
N_{lim}	System limit life, min over mechanisms	flights
N_{allow}	Operationally allowable reuse flights from Equation (6)	flights
N_{direct}	Direct-reuse boundary, $\min_i(N_{lim,i}/3)$	flights
N_{retire}	Retirement boundary, $\min_i(2N_{lim,i}/3)$	flights
$D_{op,i}$	Operational threshold of mechanism i	1/3 direct reuse; 2/3 retirement
ΔR	Contact-resistance increment of a connector	mΩ
ΔR_{lim}	Contact-resistance increment limit	5 mΩ (illustrative)
N_{cyc}, $N_{cyc,0}$	Cumulative and per-flight fretting cycle counts	cycles
N_{ref}	Reference cycle count used to anchor a	10^4 cycles (illustrative)
a, m	Power-law fitting constants of ΔR versus cycles	fitted by test
H_{env}	Environmental acceleration factor for fretting degradation	≥1; dry enclosure = 1
E_0	Initial salt/marine exposure level (new seals)	0–1
γ	Seal-aging coefficient of $E_{salt}(N)$	calibrated by test
SIR	Surface insulation resistance	Ω
ECM	Electrochemical migration	-
ACM	Atmospheric corrosion monitor	-

References

1. Long, L.; Cai, Q.; Wang, F.; Ma, T.; Wen, Y. Development of Reusable Space Transportation Technologies. *Sci. Technol. Rev.* **2018**, *36*, 84–92. (In Chinese)
2. Cao, C. *Principles of Corrosion Electrochemistry*, 3rd ed.; Chemical Industry Press: Beijing, China, 2008. (In Chinese)
3. Conseil-Gudla, H.; Staliulionis, Z.; Jellesen, M.S.; Jabbari, M.; Hattel, J.H.; Ambat, R. Humidity Buildup in Electronic Enclosures Exposed to Constant Conditions. *IEEE Trans. Compon. Packag. Manuf. Technol.* **2017**, *7*, 412–423. [CrossRef]
4. Bryant, M.D. Resistance Buildup in Electrical Connectors Due to Fretting Corrosion of Rough Surfaces. *IEEE Trans. Compon. Packag. Manuf. Technol. A* **1994**, *17*, 86–95. [CrossRef]
5. Wu, J.; Pecht, M.G. Contact Resistance and Fretting Corrosion of Lead-Free Alloy Coated Electrical Contacts. *IEEE Trans. Compon. Packag. Technol.* **2006**, *29*, 402–410. [CrossRef]
6. *IEC 60068-2 series*; Environmental Testing. International Electrotechnical Commission: Geneva, Switzerland, 2025.
7. NASA. *NASA Procedural Requirements NPR 2210.1C: Release of NASA Software—Reuse Readiness Level (RRL) Criteria*; NASA: Washington, DC, USA, 2014.
8. O'Malley, M. Qualification of Reusable Components for Launch Vehicles. In Proceedings of the Thermal & Fluids Analysis Workshop (TFAWS 2019), NASA Launch Services Program, Kennedy Space Center, Merritt Island, FL, USA, 30 August 2019. Available online: https://tfaws.nasa.gov/wp-content/uploads/TFAWS19-ID-11-Paper.pdf (accessed on 30 October 2026).
9. Fox, J.J.; Gormley, T.J. Informed Maintenance for Next Generation Reusable Launch Systems. *Acta Astronaut.* **2001**, *48*, 439–449. [CrossRef]
10. Ragab, M.M.; Cheatwood, F.M.; Hughes, S.J.; Lowry, A. Launch Vehicle Recovery and Reuse. In Proceedings of the AIAA SPACE 2015 Conference and Exposition, Pasadena, CA, USA, 31 August–2 September 2015. [CrossRef]
11. *GJB 150A-2009*; Laboratory Environmental Test Methods for Military Materiel. Chinese National Military Standard: Beijing, China, 2009. (In Chinese)
12. *MIL-STD-810H*; Environmental Engineering Considerations and Laboratory Tests. US Department of Defense: Washington, DC, USA, 2019.
13. *IPC-CC-830C*; Qualification and Performance of Electrical Insulating Compound for Printed Wiring Assemblies. IPC: Bannockburn, IL, USA, 2018.

14. Wang, N.; Miao, Y. Damage-Quantified Reusability Evaluation of Reusable Launch Vehicle Avionics: A Framework Integrating Physics-of-Failure Modeling with Multi-Criteria Decision Making. *Aerospace* **2026**, *13*, 803. [CrossRef]
15. Bahrebar, S.; Ambat, R. Time to Failure Prediction on a Printed Circuit Board Surface Under Humidity Using Probabilistic Analysis. *J. Electron. Mater.* **2022**, *51*, 4388–4406. [CrossRef]
16. Antler, M.; Drozdowicz, M.H. Fretting Corrosion of Gold-Plated Connector Contacts. *Wear* **1981**, *74*, 27–50. [CrossRef]
17. Laporte, J.; Perrinet, O.; Fouvry, S. Prediction of the Electrical Contact Resistance Endurance of Silver-Plated Coatings Subject to Fretting Wear Using a Friction Energy Density Approach. *Wear* **2015**, *330–333*, 170–181. [CrossRef]
18. Ren, W.; Wang, P.; Fu, Y.; Pan, C.; Song, J. Effects of Temperature on Fretting Corrosion Behaviors of Gold-Plated Copper Alloy Electrical Contacts. *Tribol. Int.* **2015**, *83*, 1–11. [CrossRef]
19. Jardine, A.K.S.; Lin, D.; Banjevic, D. A Review on Machinery Diagnostics and Prognostics Implementing Condition-Based Maintenance. *Mech. Syst. Signal Process.* **2006**, *20*, 1483–1510. [CrossRef]
20. Si, X.-S.; Wang, W.; Hu, C.-H.; Zhou, D.-H. Remaining Useful Life Estimation—A Review on the Statistical Data Driven Approaches. *Eur. J. Oper. Res.* **2011**, *213*, 1–14. [CrossRef]
21. van Noortwijk, J.M. A Survey of the Application of Gamma Processes in Maintenance. *Reliab. Eng. Syst. Saf.* **2009**, *94*, 2–21. [CrossRef]
22. Narayanan, G.; Golowin, A. A Stochastic Corrosion Fatigue Model for Assessing the Airworthiness of the Front Flanges of Fleet Aero Engines Using an Automated Data Analysis Method. *Corros. Mater. Degrad.* **2025**, *6*, 32. [CrossRef]
23. He, Y.; Ma, Y.; Huang, K.; Wang, L.; Zhang, J. Digital Twin Bayesian Entropy Framework for Corrosion Fatigue Life Prediction and Calibration of Bridge Suspender. *Reliab. Eng. Syst. Saf.* **2024**, *252*, 110456. [CrossRef]
24. Han, Z.; Li, X.; Chen, G. A Stochastic Model for RUL Prediction of Subsea Pipeline Subject to Corrosion-Fatigue Degradation. *Process Saf. Environ. Prot.* **2023**, *178*, 739–747. [CrossRef]
25. *ISO 9223*; Corrosion of Metals and Alloys—Corrosivity of Atmospheres—Classification, Determination and Estimation. International Organization for Standardization: Geneva, Switzerland, 2012.
26. Montgomery, E.L.; Calle, L.M.; Curran, J.C.; Kolody, M.R. *Timescale Correlation between Marine Atmospheric Exposure and Accelerated Corrosion Testing*; NASA Technical Reports Server: Hampton, VA, USA, 2012.
27. Mu, S. Analysis of Atmospheric Corrosion Environmental Factors in Wenchang Area. *Equip. Environ. Eng.* **2010**, *7*, 119–127. (In Chinese)
28. Holroyd, N.J.H.; Scamans, G.M. Stress Corrosion Cracking in Al–Zn–Mg–Cu Aluminum Alloys in Saline Environments. *Metall. Mater. Trans. A* **2013**, *44*, 1230–1253. [CrossRef]
29. Cheng, Q.; Ye, L.; Wang, S.; Gao, Q.; Xu, Y.; Xu, Y.; Chen, Y. Analysis of Cracking of 7075 Aluminum Alloy High-Lock Nuts. *Metals* **2024**, *14*, 1427. [CrossRef]
30. Eich, G.; von Czarnecki, J.; Eisenschink, C. Failure of Emergency Batteries for Aircrafts due to Stress-Corrosion Cracking. *J. Fail. Anal. Prev.* **2011**, *11*, 661–665. [CrossRef]
31. *MIL-DTL-24558A*; Terminal Boxes, Connection, for Electrical and Electronic Systems, General Specification for. U.S. Department of Defense: Washington, DC, USA, 2006.
32. *GJB 594A-2019*; Selection Principle and Thickness Series for Metallic and Chemical Coating. Equipment Development Department of CMC: Beijing, China, 2019. (In Chinese)
33. *QJ 450B-2005*; Thickness Series and Selection Principle for Metallic Coating. Commission for Science, Technology and Industry for National Defense: Beijing, China, 2005. (In Chinese)
34. *MIL-STD-889*; Dissimilar Metals. US Department of Defense: Washington, DC, USA, 2021.
35. *IPC-A-610*; Acceptability of Electronic Assemblies. IPC: Bannockburn, IL, USA, 2024.
36. *IPC-TM-650 2.3.25*; Detection and Measurement of Ionizable Surface Contaminants (ROSE/IC). IPC: Bannockburn, IL, USA, 2012.
37. *GB/T 4677.22-1988*; Test Method for Ionic Contamination on Printed Board Surfaces. Standards Press of China: Beijing, China, 1988. (In Chinese)
38. *GJB 5807-2006*; Requirements for Cleaning of Military Printed Board Assemblies after Soldering. General Armament Department of PLA: Beijing, China, 2006. (In Chinese)
39. FAA. *Acceptable Methods, Techniques, and Practices—Aircraft Inspection and Repair: AC 43.13-1B*; US Federal Aviation Administration: Washington, DC, USA, 1998.
40. *NAVAIR 01-1A-509 (series)*; Cleaning and Corrosion Control. US Naval Air Systems Command: Mary's County, MD, USA, 2005.
41. National Center for Materials Corrosion and Protection Scientific Data. Corrosion Control and Protection Technology for Carrier-Based Aircraft. 2017. Available online: https://www.corrdata.org.cn/news/science/2017-11-15/167434.html (accessed on 13 September 2026). (In Chinese)
42. *IPC-7711/7721*; Rework, Modification and Repair of Electronic Assemblies. IPC: Bannockburn, IL, USA, 2023.
43. *QJ 3259-2005*; Technical Requirements for Protective Coating of Aerospace Electronic Products. Commission for Science, Technology and Industry for National Defense: Beijing, China, 2005. (In Chinese)

44. Kömmling, A.; Jaunich, M.; Pourmand, P.; Wolff, D.; Hedenqvist, M. Analysis of O-Ring Seal Failure under Static Conditions and Determination of End-of-Lifetime Criterion. *Polymers* **2019**, *11*, 1251. [CrossRef] [PubMed]
45. *GJB 1720A-2018*; Corrosion and Protection for Dissimilar Metals. Equipment Development Department of CMC: Beijing, China, 2018. (In Chinese)
46. *GB/T 19247.1-2003*; Printed Board Assemblies—Part 1: Generic Specification. Standards Press of China: Beijing, China, 2003. (In Chinese)
47. *QJ 2850-1996*; Prevention and Control of Extraneous Matter for Aerospace Products. China Aerospace Industry Corporation: Beijing, China, 1996. (In Chinese)
48. *GB/T 2423.18-2021*; Environmental Testing—Part 2: Test Methods—Test Kb: Salt Mist, Cyclic (Sodium Chloride Solution). Standards Press of China: Beijing, China, 2021. (In Chinese)
49. *ASTM G85*; Standard Practice for Modified Salt Spray (Fog) Testing. ASTM International: West Conshohocken, PA, USA, 2019.
50. *IPC/JEDEC J-STD-033*; Handling, Packing, Shipping and Use of Moisture/Reflow Sensitive Surface Mount Devices. IPC/JEDEC: Bannockburn, IL, USA, 2018.
51. *GJB 145A-93*; Specification for Preservation Packaging. Commission for Science, Technology and Industry for National Defense: Beijing, China, 1993. (In Chinese)
52. *ANSI/VITA 46.0*; VPX Baseline Standard. VMEbus International Trade Association (VITA): Mesa, AZ, USA, 2019.
53. Steinberg, D.S. *Vibration Analysis for Electronic Equipment*, 3rd ed.; Wiley: New York, NY, USA, 2000.
54. *ISO 9224*; Corrosion of Metals and Alloys—Corrosivity of Atmospheres—Guiding Values for the Corrosivity Categories. International Organization for Standardization: Geneva, Switzerland, 2012.

Disclaimer/Publisher's Note: The statements, opinions and data contained in all publications are solely those of the individual author(s) and contributor(s) and not of MDPI and/or the editor(s). MDPI and/or the editor(s) disclaim responsibility for any injury to people or property resulting from any ideas, methods, instructions or products referred to in the content.